NINETEENTH EUROPEAN ROTORCRAFT FORUM

Paper n° C14

A BOUNDARY INTEGRAL FORMULATION FOR THE AERODYNAMIC ANALYSIS OF PARALLEL BLADE-VORTEX INTERACTIONS OVER AEROFOILS

by

A. VISINGARDI
CIRA, ITALY

September 14-16, 1993
CERNOBBIO (Como)
ITALY

ASSOCIAZIONE INDUSTRIE AEROSPAZIALI
ASSOCIAZIONE ITALIANA DI AERONAUTICA ED ASTRONAUTICA

A BOUNDARY INTEGRAL FORMULATION FOR THE AERODYNAMIC ANALYSIS OF PARALLEL BLADE-VORTEX INTERACTIONS OVER AEROFOILS

A. Visingardi

CIRA, Centro Italiano Ricerche Aerospaziali
81043 Capua, Italy

ABSTRACT

A boundary integral formulation for the analysis of the non-impinging parallel BVI problem over aerofoils, for both incompressible and subsonic compressible flows, is described and validated in the present paper. In the incompressible analysis the formulation is compared to a Discrete Vortex Method. The results obtained by the compressible analysis are compared with those obtained by Euler, Thin-Layer N.S. and the ATRAN2 T.S.D. codes. There is generally a satisfactory agreement between the present method and the others.

1. INTRODUCTION

Blade-vortex interactions (BVI) occur in helicopter rotors when a rotor blade passes in the vicinity or through a tip vortex trailing from the same or the preceding blade. Depending on the flight conditions, these interactions determine a strong variation in the loading that can be confined to the blade tip, for the case of hover, or extending to the entire rotor disk as for manoeuvers, low-speed forward flight and low-power descending flight. As a result of such vortex-induced variations in the loading, rotor higher harmonic loads and vibrations arise. Furthermore, they are considered as one of the mechanisms responsible for the high frequency noise, commonly referred as "blade slap" [1].

The general blade-vortex interaction problem is three-dimensional and unsteady, and the curved-line vortex intersects the blade at various angles. Although oblique interactions represent the helicopter application more closely, two limiting cases of interactions are of fundamental interest. One limiting case occurs when the axis of the vortex is parallel to the blade leading edge, fig. 1a. The interaction is two-dimensional, the vortex is convected past the blade with the free stream and the problem is therefore highly unsteady. Another occurs when the axis of the vortex is normal to the blade leading edge, fig. 1b. This interaction is highly three-dimensional but steady and no noise is therefore generated. Since a parallel interaction affects a larger span of the blade than a perpendicular interaction, it is reasonable to expect that a model for the parallel interaction is more crucial to predicting blade forces and moments during blade-vortex interactions.

The parallel BVI problem was first looked at by Sears [2] using classical, incompressible, two-dimensional unsteady linear aerofoil theory. The lift on the blade was calculated from the gust-entry lift function of von Karmann and Sears [3] using Duhamel superposition. The vortex was kept at a constant vertical distance from the blade during the encounter. Parthasarathy [4], and Chow and Huang [5] have solved the incompressible problem using conformal mapping techniques in which the vortex is convected at the local velocity. Conformal mapping techniques have also been used by Meyer and Timm [6], Panaras [7], and Poling et alii [8]. Renzoni et alii [9,10,11] have solved the problem by a discrete free-vortex modelling of the vortex and wake based on the classical

incompressible, potential flow theory. A panel method has been used by Wu et alii [12,13] to solve the full Navier-Stokes equations in the vorticity-stream function form for incompressible viscous interactions. The parallel interaction problem was first analysed in transonic flow by Caradonna et alii [14], and McCroskey and Goorjian [15] using unsteady transonic small disturbance theory. Jones [16], and Sankar and Malone [17] have modelled the interaction more accurately by applying the full potential equation without small disturbance and low-frequency assumptions. Srinivasan et alii [18,19,20], and Wu et alii [13] have developed more advanced interaction models by solving the unsteady, time-averaged, compressible Navier-Stokes equations. All of the methods described above are either incompressible or, when compressible, are rather time consuming. Such methods cannot yet very conveniently be extended to the analysis of the real three-dimensional, unsteady BVI problem. Furthermore, for most of them, the accurate description of the wake is a problem still open.

The present paper describes a boundary-integral formulation for the analysis of the non-impinging parallel BVI problem over aerofoils in incompressible and subsonic compressible flow. It is a first step toward the analysis of the general BVI problem on helicopter rotors. Morino's B.E.M. code MODAIR HR-0 has been modified to take into account the presence of the vortex and the results obtained have been compared with other numerical formulations.

2. INTEGRAL FORMULATION

The governing equation for potential compressible flows, written in a body frame of reference (BFR, fixed with the aerofoil), is given by

$$\nabla^2\phi - \frac{1}{a^2_\infty}\left(\frac{\partial}{\partial t} + U_\infty \frac{\partial}{\partial x}\right)^2 \phi = \sigma \qquad x \text{ outside } \mathcal{S}(t) \tag{1}$$

where ϕ is the velocity potential such that $\mathbf{v} = \nabla\phi$ and σ indicates the nonlinear terms that are important only in transonic regime. $\mathcal{S}(t)$ is a surface outside of which the flow is potential and it consists of a surface $\mathcal{S}_B$ surrounding the aerofoil, a surface $\mathcal{S}_W$ surrounding the wake and a surface $\mathcal{S}_V$ surrounding the vortex. The boundary condition at infinity is that $\phi = 0$. The surface $\mathcal{S}_B$ of the aerofoil is assumed to be impermeable hence $\partial\phi/\partial n = (\mathbf{v}_B - U_\infty \mathbf{i}) \cdot \mathbf{n}$ where $\mathbf{v}_B$ is the velocity of a point on the aerofoil and U_∞ the free stream velocity. The wake is a surface of discontinuity which is not penetrated by the fluid and across which there is no pressure jump. The second wake condition implies that $\Delta\phi$ remains constant following a wake point $\mathbf{x}_W$, and equal to the value it had when $\mathbf{x}_W$ left the trailing edge. The value of $\Delta\phi$ at the trailing edge is obtained by using the Kutta-Joukowski hypothesis that no vortex filament exists at the trailing edge; this implies that the value of $\Delta\phi$ on the wake and the value of $\Delta\phi$ on the body are equal at the trailing edge [21].

Applying the Green's function method to Eq. (1), neglecting the nonlinear terms ($\sigma = 0$), yields the following boundary-integral-representation for the velocity potential ϕ

$$E(\mathbf{x}_*)\phi(\mathbf{x}_*, t_*) = I_B + I_W + I_V \tag{2}$$

with

$$I_B = \oiint_{S_B} \left\{ \left(\frac{-1}{4\pi\hat{\varrho}}\right) \frac{\partial\phi}{\partial\tilde{n}} - \phi \frac{\partial}{\partial\tilde{n}}\left(\frac{-1}{4\pi\hat{\varrho}}\right) + \left(\frac{-1}{4\pi\hat{\varrho}}\right) \frac{\partial\phi}{\partial t}\left(\frac{\partial\theta}{\partial\tilde{n}} + 2\frac{\mathbf{M}\cdot\mathbf{n}}{\mathbf{a}_\infty}\right) \right\}_{t_*-\theta} dS$$

$$I_W = \iint_{S_W} \left\{ -\Delta\phi \frac{\partial}{\partial\tilde{n}}\left(\frac{-1}{4\pi\hat{\varrho}}\right) + \left(\frac{-1}{4\pi\hat{\varrho}}\right) \frac{\partial\Delta\phi}{\partial t}\left(\frac{\partial\theta}{\partial\tilde{n}} + 2\frac{\mathbf{M}\cdot\mathbf{n}}{\mathbf{a}_\infty}\right) \right\}_{t_*-\theta} dS$$

$$I_V = -\Gamma \iint_{S_V} \left[\frac{\partial}{\partial\tilde{n}}\left(\frac{-1}{4\pi\hat{\varrho}}\right) \right]_{t_*-\theta} dS$$

representing respectively the contribution of the aerofoil, the wake and the interacting vortex. $E(\mathbf{x}_*)$ is a domain function defined as zero inside S and unity everywhere else, Γ represents the circulation of the vortex. Furthermore, $\partial/\partial\tilde{n} = \partial/\partial n - \mathbf{M}\cdot\mathbf{n}\mathbf{M}\cdot\nabla$, $\hat{\varrho} = [\varrho|1+\mathbf{M}\cdot\boldsymbol{\varrho}/\varrho|]_{t_*-\theta}$, $\varrho = ||\boldsymbol{\varrho}|| = ||\mathbf{x}-\mathbf{x}_*||$ and $\mathbf{M} = -U_\infty \mathbf{i}/a_\infty$, the Mach vector. The integrals are evaluated at $t = t_* - \theta$ where $\theta = \varrho/a_\infty$ is the time required for a signal emitted in $\mathbf{x}$ to arrive in $\mathbf{x}_*$.

From a physical point of view, Eq. (2) can be interpreted as follows: the effect of the presence of the aerofoil can be simulated by replacing the aerofoil with a layer of sources on its surface plus a layer of doublets and rate doublets, also called "ratelets", on the surfaces of the aerofoil and the wake. Furthermore, the effect of the presence of a vortex in the flowfield is simulated by replacing the vortex with a doublet.

The wake is modelled either by a "prescribed wake" modelling or by a "free wake modelling". With the first the wake is simply a surface generated by the aerofoil trailing edge during its motion at the free stream velocity and therefore its shape is assigned. In the free wake modelling, used only in the incompressible analysis, the influences of the aerofoil, the vortex and the wake itself are taken into account to determine the wake shape. A new position of the wake points is determined at each time step by knowing their position and velocity in the previous time step. Thus, the wake geometry is not known a priori and constitutes an integral part of the aerodynamic problem.

An expression of the wake node velocities is obtained by taking the gradient of Eq. (2) in its incompressible form

$$\mathbf{v}_* = \nabla_*(E_*\phi_*) = \oint\!\!\!\!\!\!\iint_{S_B} \left\{ \nabla_* \left(\frac{-1}{4\pi\varrho}\right) \frac{\partial\phi}{\partial n} - \nabla_* \left[\frac{\partial}{\partial n}\left(\frac{-1}{4\pi\varrho}\right)\right]\phi \right\} dS$$
$$- \iint_{S_W} \nabla_* \left[\frac{\partial}{\partial n}\left(\frac{-1}{4\pi\varrho}\right)\right] \Delta\phi\, dS - \Gamma \iint_{S_V} \nabla_* \left[\frac{\partial}{\partial n}\left(\frac{-1}{4\pi\varrho}\right)\right] dS \qquad (3)$$

Once the velocities are computed the new location of the wake nodes is given by

$$\mathbf{x}_*(t_* + dt) = \mathbf{x}_*(t_*) + \mathbf{v}_*(\mathbf{x}_*, t_*)dt \qquad (4)$$

A Rankine vortex core model is used in order to avoid numerical instabilities in the wake. The velocity induced by a potential vortex is corrected as $v = \alpha\frac{\Gamma}{2\pi r}$ where $\alpha = r^2/\epsilon^2$ for $r \leq \epsilon$, being ϵ the vortex core radius, and $\alpha = 1$ elsewhere.

The same procedure has been followed for the computation of the free vortex path. In particular, the compressibility effects on the path have been computed by correcting the incompressible velocity as follows

$$v_{comp} = v_{incomp} \frac{\beta}{\cos^2\theta + \beta^2 \sin^2\theta} \qquad (5)$$

with $\beta = \sqrt{1 - M_\infty{}^2}$ and θ the inclination between the velocity vector and the axis normal to the aerofoil chord.

A zeroth-order boundary element method (BEM) is used for the discretization of the integral equation, Eq. (2). The surface of the aerofoil and of the wake are divided into hyperboloidal quadrilateral elements. The vortex is explicitly modelled by a single panel of very high length extending from the vortex position to the far field. ϕ, $\partial\phi/\partial\tilde{n}$, $\Delta\phi$ are assumed constant over each element. Using the collocation method and setting the collocation points at the centroid of each element on the aerofoil, leads to a differential-delay equation for the velocity potential ϕ which in matrix form is

$$[\mathbf{A}]\{\phi\} = \{\mathbf{b}\} \qquad (6)$$

where [**A**] is the matrix of influence coefficients at the current time t, $\{\phi\}$ is the vector of unknown velocity potentials, and $\{\mathbf{b}\}$ is a vector of terms known at time t. The elements of [**A**] and $\{\mathbf{b}\}$ are calculated analytically. The above system of simultaneous linear algebraic equations is solved for the unknown vector $\{\phi\}$ by inverting [**A**].

The collocation method is then applied again in order to obtain a discretized expression for the wake nodes and vortex velocities.

3. RESULTS AND DISCUSSION

The parallel encounter between a helicopter blade tip-vortex in forward flight and the following blade can be approximated by the unsteady, two-dimensional interaction of a concentrated vortex with a stationary aerofoil. In the present paper such an interaction is considered between a potential vortex and Joukowski and NACA 0012 aerofoils. The present method is validated on a test case that has been extensively studied by other investigators.

The incompressible BVI analysis is performed on the Joukowski aerofoil and the results are compared with those obtained by Renzoni's Discrete Vortex Method (D.V.M.) code [9] based on a discrete free-vortex modelling of the vortex and wake within the framework of classical incompressible, potential flow theory. The subsonic, compressible BVI analysis is performed on the NACA 0012 aerofoil and the results are compared with those obtained by Srinivasan's Euler and Thin-Layer Navier Stokes codes [19,20] and McCroskey's Transonic Small Disturbances (T.S.D.) ATRAN2 code [19,20].

Two kinds of vortex interactions are considered. In the first case, called "forced-interaction", the vortex is convected downstream along a prescribed path with the free stream velocity. In the second case, called "force-free interaction", the vortex is convected downstream along a force-free path with the local velocity of the flow.

The aerofoil is discretised by 80 panels and set at zero angle of attack so that no lift would be generated in absence of the vortex. The wake, extending 10 chords downstream of the T.E., is discretised by 60 panels. The interacting vortex, having a nondimensional circulation of Γ =0.2 (positive in the clockwise direction) is initially positioned 0.26 chords below the aerofoil and 5 chords upstream (x_v/c =-5, y_v/c =-0.26). In order to save computational time and to have a higher level of accuracy only in the vicinity of the aerofoil, where the BVI effects are stronger, a variable time step is used. Therefore, a $\Delta t = 0.10$ is used from upstream (x_v/c =-5) to one chord ahead of the aerofoil and from one chord behind it to further downstream ($x_v/c \simeq 5$). A $\Delta t = 0.05$ is used in the remaining part of the vortex path ($-1 < x_v/c < 1$).

The code has been run on a CONVEX C3860 computer in vectorial mode. Typical average computational times expressed as CPU time are as follows: BVI with prescribed wake = 80 sec and BVI with free wake = 1000 sec. No significant differences have been observed between incompressible and compressible analysis.

3.1 *Incompressible BVI analysis - Joukowski aerofoil*

During a vortex interaction the flowfield around an aerofoil is subjected to changes that strongly influence the path of the vortex itself. In fig. 2a the result of such an influence is shown. The altered flowfield of the aerofoil induces a downwash increasingly stronger as the vortex approaches the L.E. (leading edge) so that it is pushed down while moving downstream along a force-free path (F.P.). Once under the aerofoil the flowfield induces an upwash and the vortex is pushed up. Beyond the T.E. (trailing edge), the vortex interacts with the wake. Depending on the wake modelling two different effects can be observed. In the "prescribed-wake" modelling (P.W.) the upwash is still quite strong and the vortex is convected downstream on a rising path. In the

"free-wake" modelling (F.W.) the upwash is sensibly reduced. This can be explained by the fact that now the wake, free to move, is able to partially absorb the effects of the main vortex determining, in this way, a weaker influence on the vortex itself. The case of a "prescribed-vortex path" interaction with a "prescribed-wake" modelling (P.P, P.W.) is shown for completeness. In this case the aerofoil flowfield has no effect on the vortex since its path is assigned.

In fig. 2b the vortex interaction in terms of C_l is shown. When the vortex is in front of the aerofoil, it determines a downwash effect giving as a result a negative value of the effective angle of attack which in turn causes a negative lift. While moving under the aerofoil, the effect changes, the upwash that the vortex now determines gives a positive effective angle of attack and so the lift becomes positive. The vortex position and especially its rate of change, determines the most dramatic effect in about one chord around the aerofoil, as shown in the figure. The use of a P.P. or a F.P. with a P.W. or a F.W. shows no differences on the C_l. The only exceptions occur around the L.E., where the P.P., being closer to the aerofoil with respect to the F.P., determines a higher negative lift, and around the T.E. where the P.P. determines a slightly lower lift. The P.P. also determines a slightly higher C_d, fig. 2c, whereas the $C_{m_{L.E.}}$ shows a tendency to overestimate the pitch-up and to underestimate the pitch-down, fig. 2d.

In fig. 3 is shown a comparison of results obtained by B.E.M. and those obtained by a D.V.M. code, using for both methods a F.P., F.W. modelling. Fig. 3a shows the comparison in terms of C_l. The agreement is fairly satisfactory even though the local change in slope that occurs in the D.V.M. results around the T.E. is not present in the B.E.M. results determining, in this way, a considerable gap between the two. Some discrepancies are also present in fig. 3b where the C_d diagram is shown. The drag coefficient computed by B.E.M. is overestimated almost everywhere with respect to D.V.M.. In figs. 3c and 3d are then shown the C_m diagrams respectively referred to the L.E. and to $c/4$. Considerable differences are observed. Even the smallest differences in terms of C_l and C_d are amplified, especially for the $C_{m_{c/4}}$ that is usually the most difficult to predict correctly. In particular, the change in the concavity present around the middle of the aerofoil in the D.V.M. results of fig. 3c is hardly visible in the B.E.M. results, and also positioned toward the L.E.. Such a difference is then observed more evidently in fig. 3d where an inversion of C_m between the two methods is present around the T.E..

Fig. 3e presents a comparison between the vortex paths obtained by using the two different methods. It can be seen that, the wake modelling determines great differences. The analysis performed with the D.V.M., using a "free-wake" modelling (F.W.), compared with that one performed by D.V.M., using a "prescribed-wake" modelling (P.W.) puts into evidence the same behaviour noticed in fig. 2a for the B.E.M. results in the same conditions. However, the effect here is much more dramatic even determining an inversion in the path.

A comparison of C_p between the two methods in four different locations of the vortex is shown in fig. 4. The agreement in all four cases is quite satisfactory. A general consideration that can be drawn is that the pressure distribution on the upper part of the aerofoil is rather insensitive to the presence of the vortex, remaining more or less the same for all the locations. The passage of the vortex under the aerofoil is shown by the presence of a small kink that arises on the lower part of the C_p at x_v/c =0.50, fig. 4c. While moving downstream, the vortex determines first a higher suction effect on the lower part of the aerofoil and then on the upper part with the result that the lift from the negative value becomes positive. In fig. 4d is shown the C_p at x_v/c =1.0. Here the two methods show some differences. In the D.V.M. the C_p intersects about at the mid-chord whereas with B.E.M. this effect doesn't occur showing just a gap at the T.E..

3.2 *Compressible BVI analysis - NACA 0012 aerofoil*

The effects of a subsonic compressible BVI are analysed by B.E.M. using both a P.P., P.W. modelling and a F.P., P.W. modelling. In particular, in fig. 5 are shown the results obtained with the

F.P., P.W. modelling. In fig. 5a the effects of compressibility on C_l determines an increase, in absolute value, in the lift at the L.E. and T.E., and a decrease just after the T.E. to further downstream. The higher is the Mach number, the stronger this effect is felt. In particular, compressibility seems to accelerate the process of restoring the initial condition of C_l =0 that was present far upstream.

During the study, a problem arose while increasing the Mach number. Some numerical instabilities have been observed on the solution. An analysis of the problem has localised the source of such instabilities in the ratelet terms. Furthermore, it has been observed that the problem could be reduced, at a given Mach number, by increasing the time step but losing, in this way, accuracy in capturing the real unsteadiness of the problem. This solution has been applied for the case at M =0.5. The extremely high value of C_l observed in this case around the T.E. can therefore be explained as the result of a not-fully unsteady treatment of the problem.

Fig. 5b shows the C_d behaviour. In this case compressibility also determines an increase in magnitude. The computation of the pitching moment around the L.E. shows instead that not only it is increased by compressibility but also that the inflection point, that is present about at the mid-chord when M =0, moves toward the L.E. and to the zero value of C_m, fig. 5c. A different behaviour is shown for $C_{m_{c/4}}$, fig. 5d. In this case, compressibility first reduces the strength, M =0.3, and then determines an inversion of the whole curve.

An important role is played by compressibility also on the vortex path. As can be observed in fig. 5e, the path after the T.E. tends to rise with a higher slope as the Mach number increases. Furthermore, it is also clear that compressibility influences in a greater way the wake since the differences in the vortex path are more evident in the region where the interaction between the vortex and the wake is stronger.

A comparison between B.E.M. results and those obtained by Srinivasan and McCroskey [19,20] is also performed. A Mach number equal to M =0.3 is considered and the analysis is performed by using a P.P., P.W. modelling. In fig. 6a is represented the C_l diagram. The agreement is generally satisfactory. However, B.E.M. result shows a higher negative value of the lift around the L.E. whereas, around the T.E., the local change in slope that occurs is not followed by the other methods. Finally, just after the T.E., it is important to notice how close is the agreement of the present method with the T.S.D. ATRAN2 results.

In fig. 6b is shown the comparison in terms of $C_{m_{c/4}}$. Here, once again, the difficulty in predicting correctly the moment coefficient is evident. The agreement can be considered sufficient up to the L.E. After it, the main differences appear. In particular, the gap present in the C_l curve around the T.E. between B.E.M. and the other methods reflects itself in determining a pitch-up instead of a pitch-down moment.

A C_p comparison between B.E.M. and T.S.D. ATRAN2 results for four different locations of the vortex is shown in fig. 7. When x_v/c =-0.50 and x_v/c =0.0, figs. 7a, 7b, the C_p for both the methods follows the same behaviour even though B.E.M. results are such that the corresponding lift is more negative, especially when x_v/c =0.0. Once the vortex reaches the position x_v/c =0.50, fig. 7c, it can be observed that the C_p distribution in the upper part of the aerofoil is in practice the same whereas the kink in the B.E.M. results, indicating the presence of the vortex, is not captured by the T.S.D. method. However, the corresponding lift is equal for both the methods. Under the T.E., fig. 7d, the C_p distribution on the upper part remains the same as in the previous case. In the lower part, instead, B.E.M. tends to overestimate the suction effect giving as a result a smaller lift than that obtained in T.S.D. As in the incompressible case, the vortex determines big differences only on the lower part of the aerofoil, leaving the upper part almost unaltered.

4. CONCLUDING REMARKS

The aim of the paper has been the analysis of a boundary integral formulation approach to the non-impinging, parallel BVI over aerfoils. The study of this phenomenology, two-dimensional but strongly unsteady, is intended as a first step of fundamental importance toward the prediction of blade forces and moments that arise during the real three-dimensional and unsteady BVI problem that takes place on helicopter configurations especially during low-speed forward and descent flight.

Morino's MODAIR HR-0 B.E.M. code has been modified for an incompressible and subsonic compressible analysis of the parallel BVI problem. The results obtained by the incompressible analysis have been compared with Renzoni's Discrete Vortex Method. The agreement has been generally satisfactory. Some significant differences have been observed in the $C_{mc/4}$ comparison. The free wake modelling of D.V.M. has shown a stronger effect on the vortex path than that observed by B.E.M. free wake modelling.

In the compressible analysis, numerical instabilities have arisen that amplify with increasing Mach number and/or decreasing time step. Such a problem, caused by the ratelet terms, has limited the applicability of the method to Mach numbers at or below $M = 0.5$. The solution of this problem is of primary importance. The comparison with Srinivasan's Euler and Thin-Layer N.S. codes, and McCroskey's ATRAN2 T.S.D. code has shown a good agreement also for compressible BVI. However, also in this case significant differences have been observed in the $C_{mc/4}$ comparison. This problem has again put into evidence the difficulty of correctly predicting the $C_{mc/4}$.

The simplicity with which the boundary integral formulation allows the modelling of the BVI phenomenology, together with the encouraging results obtained to date, makes the present method a promising tool for the understanding of the aerodynamic aspects of the problem and for providing reliable data to the aeroacousticians for the noise prediction.

ACKNOWLEDGEMENTS

The author is very grateful to P. Renzoni of CIRA for providing his precious results and many useful suggestions.

REFERENCES

1. W. Johnson, Helicopter Theory, Princeton University Press, 1980.

2. W.R. Sears, Aerodynamics, Noise, and the Sonic Boom, AIAA Journal, Vol. 7, No. 4, pp. 577-586, 1969.

3. T. von Karman and W.R. Sears, Airfoil Theory for Non-Uniform Motion, Journal of the Aeronautical Sciences, Vol. 5, No. 10, pp. 379-390, 1938.

4. R. Parthasarathy, Aerodynamic Sound Generation due to Vortex-Airfoil Interaction, Ph. D. Dissertation, Stanford Univ., Stanford, CA, 1972.

5. C.Y. Chow and M.K. Huang, Unsteady Flows about a Joukowsky Airfoil in the presence of Moving Vortices, AIAA Paper 83-0129, January 1983.

6. G.E.A. Meyer and R. Timm, Unsteady Vortex Airfoil Interaction, AGARD CP-386, 1985.

7. A.G. Panaras, Numerical Modeling of the Vortex/Airfoil Interaction, AIAA Journal, Vol. 25, No. 1, pp. 5-11, 1987.

8. D.R. Poling, L. Dadone and D.P. Telionis, Blade-Vortex Interaction, AIAA Paper 87-0497, January 1987.

9. P. Renzoni, Discrete Vortex Modeling of a Blade-Vortex Interaction, Ph.D. Thesis, Rensselaer Polythecnic Institute, Troy, N.Y., 1987.

10. J. Straus, P. Renzoni and R.E. Mayle, Airfoil Pressure Measurements During a Blade-Vortex Interaction and a Comparison with Theory, AIAA Journal, Vol.28, No. 2, February 1990.

11. P. Renzoni and R.E. Mayle, Incremental Force and Moment Coefficients for a Parallel Blade-Vortex Interaction, AIAA Journal, Vol.29, No. 1, January 1991.

12. J.C. Wu, L.N. Sankar and T.M. Hsu, Unsteady Aerodynamics of an Airfoil Encountering a Passing Vortex, AIAA Paper 85-0203, January 1985.

13. J.C. Wu, T.M. Hsu, W. Tang and L.N. Sankar, Viscous Flow Results for the Vortex-Airfoil Interaction Problem, AIAA Paper 85-4053, October 1985.

14. F.X. Caradonna, A. Desopper and C. Tung, Finite-Difference Modeling of Rotor Flows Including Wake Effects, NASA TM-84280, 1982.

15. W.J. McCroskey and P.M. Goorjian, Interactions of Airfoils with Gust and Concentrated Vortices in Unsteady Transonic Flow, AIAA Paper 83-1691, July 1983.

16. H.E. Jones, The Aerodynamic Interaction Between an Airfoil and a Vortex in Transonic Flow, Workshop on Blade-Vortex Interactions, NASA Ames Research Center, October 1984.

17. L.N. Sankar and J.B. Malone, Unsteady Transonic Full Potential Solutions for Airfoils Encountering Vortices and Gusts, AIAA Paper 85-1710, July 1985.

18. G.R. Srinivasan, W.J. McCroskey and P. Kutler, Numerical Simulation of the Interaction of a Vortex with a Stationary Airfoil in Transonic Flow, AIAA Paper 84-0254, January 1984.

19. G.R. Srinivasan, Computations of Two-Dimensional Airfoil-Vortex Interactions, NASA CR 3885, May 1985.

20. G.R. Srinivasan and W.J. McCroskey, Numerical Simulations of Unsteady Airfoil-Vortex Interactions, Vertica, Vol. 11, No. 1/2, pp. 3-28, 1987.

21. L. Morino and K. Tseng, A General Theory of Unsteady Compressible Potential Flows with Applications to Airplanes and Rotors, Eds: P.K. Banerjee and L. Morino, Developments in Boundary Element Methods, Volume 6: Nonlinear Problems of Fluid Dynamics, Elsevier Applied Science Publisher, Barking, UK, 1990.

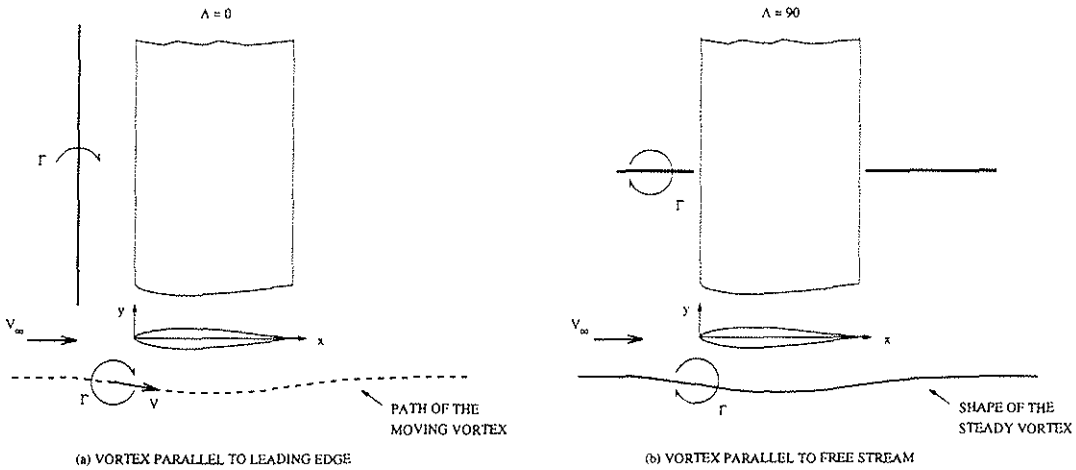

Figure 1.: Limiting cases of the blade-vortex interaction problem.

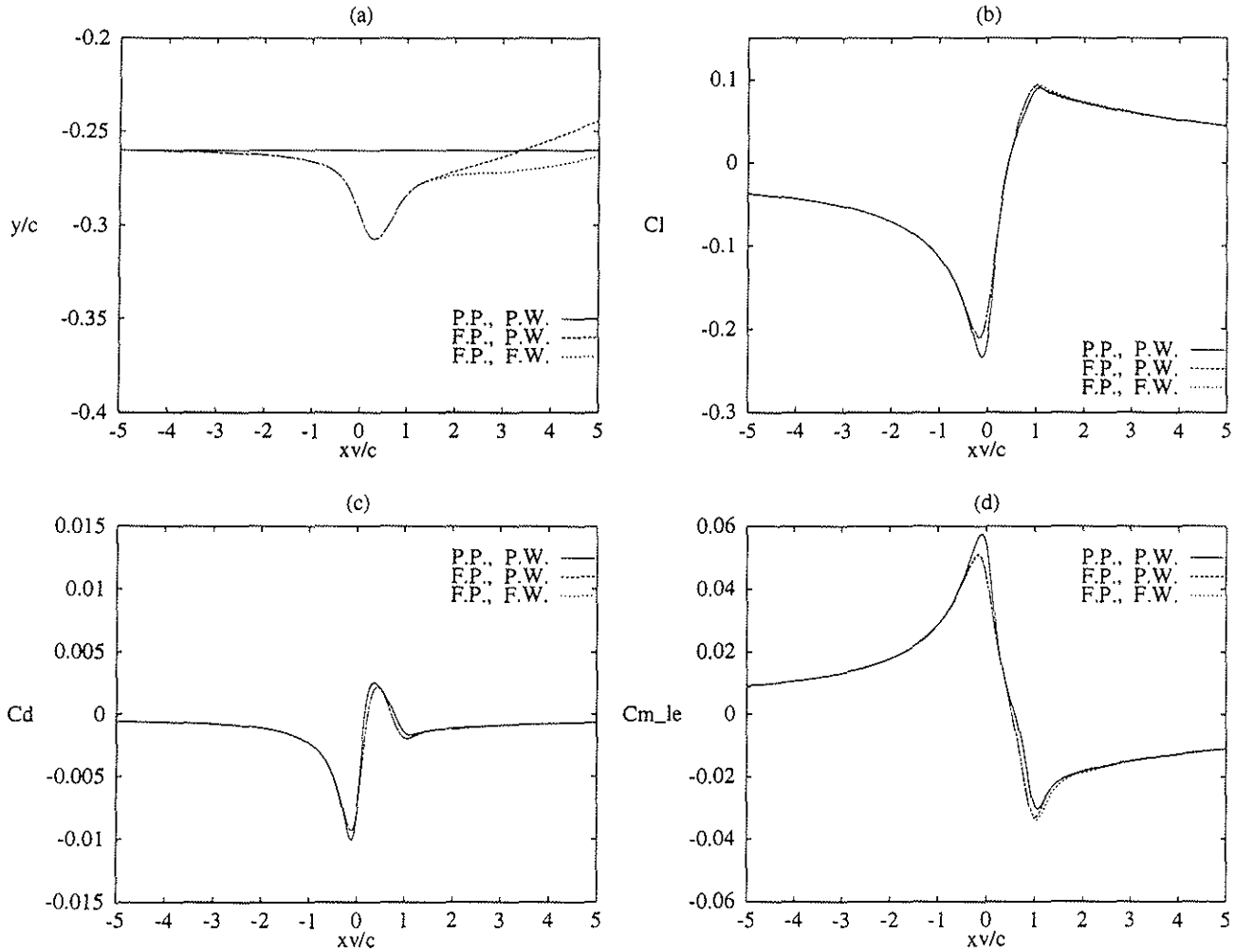

Figure 2.: B.E.M. results with different wake and vortex modelling. Joukowski, $M = 0.$, $\alpha = 0.$, $\Gamma = 0.2$, $x_o = -5.$, $y_o = -0.26$

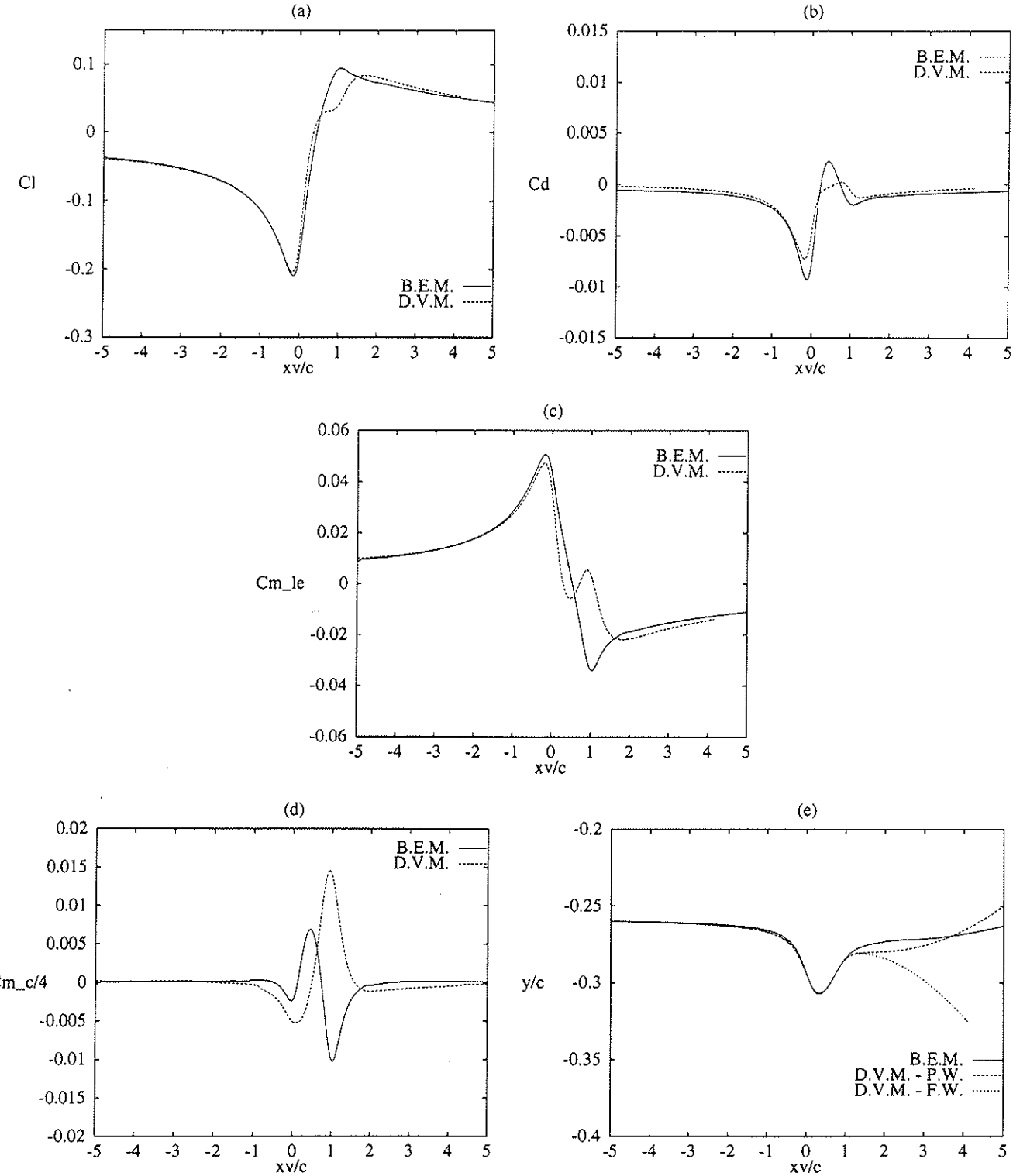

Figure 3.: Comparison between B.E.M. and D.V.M. results: Joukowski, $M = 0.$, $\alpha = 0.$, $\Gamma = 0.2$, $x_o = -5.$, $y_o = -0.26$

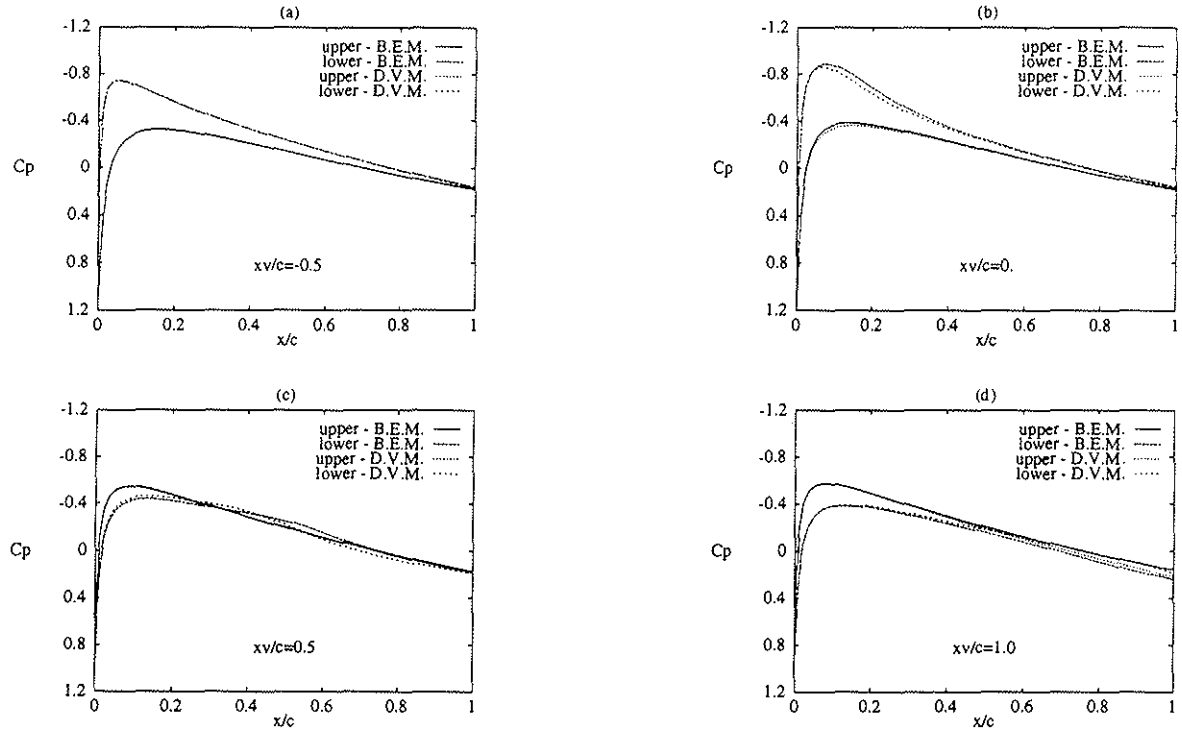

Figure 4.: Cp comparison between B.E.M. and D.V.M. results: Joukowski, $M = 0.$, $\alpha = 0.$, $\Gamma = 0.2$, $x_o = -5.$, $y_o = -0.26$

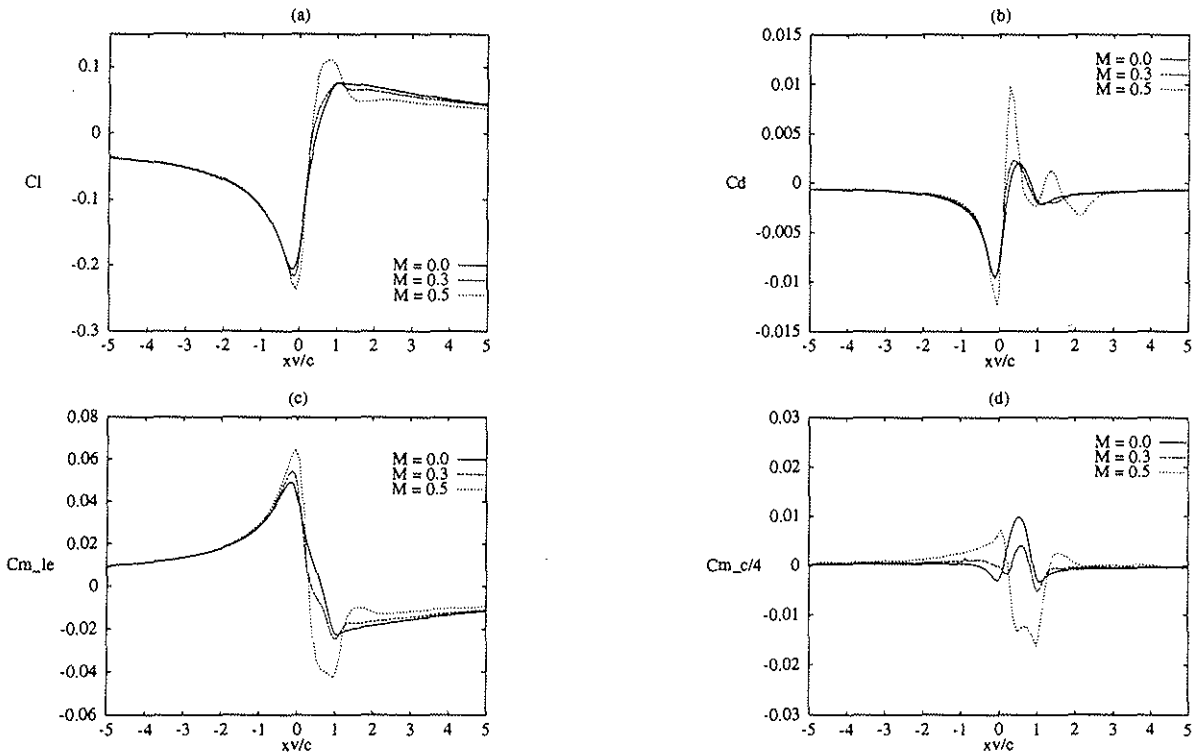

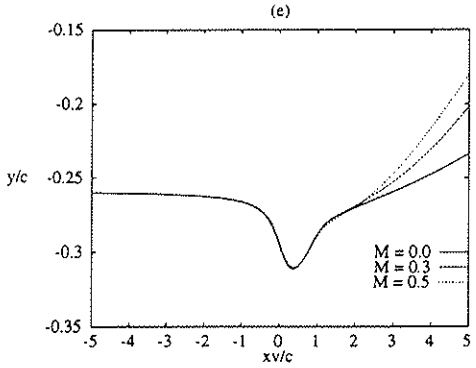

Figure 5.: Compressibility effects on B.E.M. results: NACA 0012, $\alpha = 0.$, $\Gamma = 0.2$, $x_o = -5.$, $y_o = -0.26$

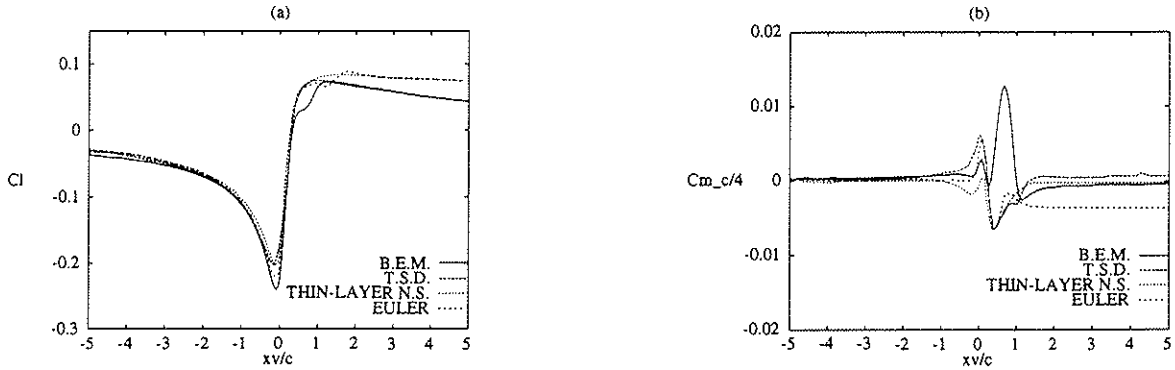

Figure 6.: Lift and pitching-moment coefficient comparison between B.E.M. and other methods: NACA 0012, $M = 0.3$, $\alpha = 0.$, $\Gamma = 0.2$, $x_o = -5.$, $y_o = -0.26$

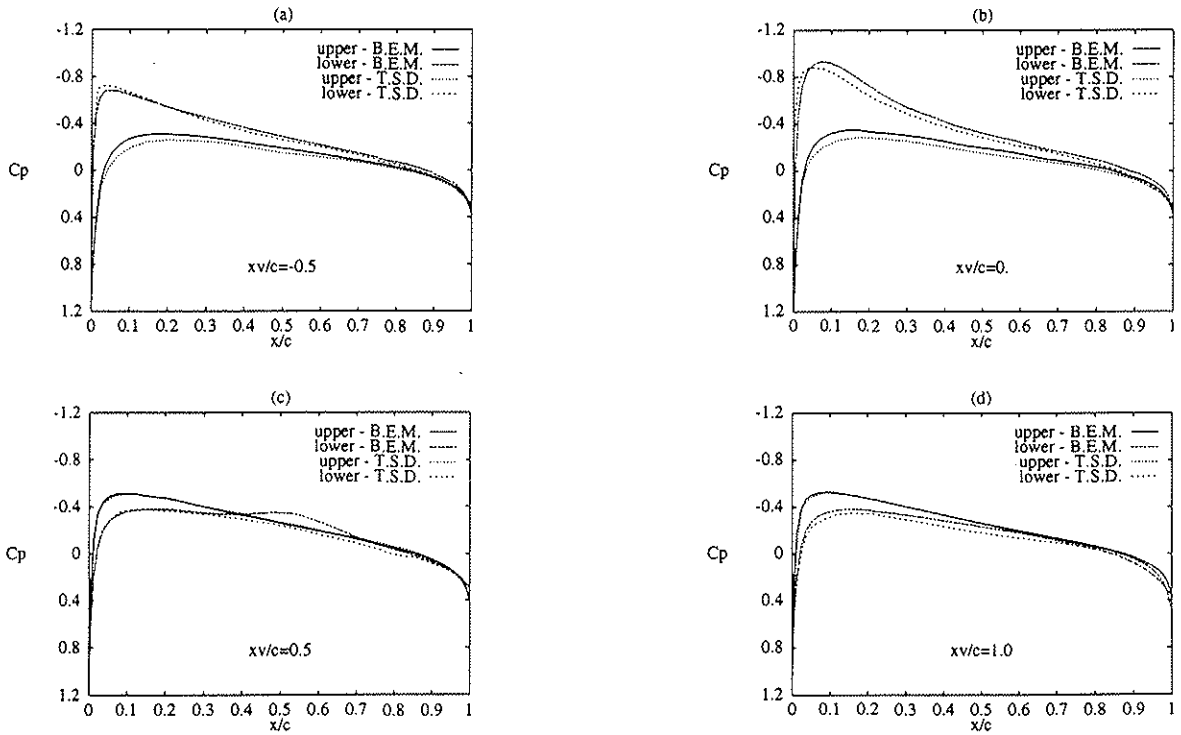

Figure 7.: Cp comparison between B.E.M. and T.S.D. results: NACA 0012, $M = 0.3$, $\alpha = 0.$, $\Gamma = 0.2$, $x_o = -5.$, $y_o = -0.26$